RF Spectrum of a Signal after Frequency Multiplication; Measurement and Comparison with a Simple Calculation

FRED L. WALLS AND ANDREA DEMARCHI

Abstract—**A novel experimental technique is introduced and used to measure the effect of frequency multiplication on the RF spectrum of an oscillator. This technique makes it possible to produce the RF spectrum at *X* band—where measurements are relatively straightforward—that would have been produced by frequency multiplication of the 5-MHz source to any frequency from 9.2 GHz to 100 THz (10^{14} Hz). A simplified theory is developed and shown to reproduce the experimental results for the relative power in the carrier and noise pedestal, and the shape and the width of the carrier and noise pedestal, to within the measurement uncertainty of 2 or 3 dB, from 5 MHz to 10 THz. The calculations are easily made using analytical techniques from the measurement of the spectral density of phase fluctuations of the source, the effective input spectrum density and the bandwidth of the multiplier chain, and the frequency multiplication factor. It is shown that present 5-MHz-crystal-controlled oscillators are useful as a precision source to ~500 GHz. Suggestions for extending their range to ~100 THz are made.**

INTRODUCTION

FREQUENCY multiplication by large factors imposes very severe requirements on the RF spectrum of the source and the first few steps of the multiplication chain if the resulting RF spectrum is to be very narrow. This is because the power in the noise sidebands relative to the carrier generally increase as n^2, where n is the multiplication factor, until all the power is in the sidebands [1]–[4].

The purpose of this paper is to present experimental measurements and a simplified theory which show in detail how the RF spectrum is modified by the frequency-multiplication process. To accomplish this, two precision 5-MHz-crystal-controlled oscillators are used as sources for multiplication to 9.2 GHz. One of the oscillators is equipped with a phase modulator so that additional amounts of white phase noise can be added to the signal. Since the noise sidebands or noise pedestal of this and many other precision crystal-controlled oscillators is dominated by white phase noise, this process simulates the effect of frequency multiplication on the noise pedestal. Phase measurements between the two oscillators are made before and after multiplication by 1836 to 9.2 GHz. In this way, it is easy to measure the ratio of power in the carrier to power in the noise pedestal, and the shape of the pedestal as a function of total phase modulation. This novel technique allows one to evaluate the ultimate performance of a signal source after synthesis to frequencies ranging up to 100 THz (10^{14} Hz) without actually having to build 100-THz-multiplier chains. A method for determining the noise in the multiplier chain and its effect on the RF spectrum is also given.

Comparison with the experimental measurements show that several relatively simple expressions, which can be easily evaluated analytically, are sufficient to calculate the relative power in the carrier and the noise pedestal, and the width and shape of the carrier and the noise pedestal over a wide range of total phase modulation or multiplication factors. This simplified theory uses the measurement of the spectral density of phase fluctuations of the source, the equivalent added noise and the bandwidth of the multiplier chain, and the multiplication factor n to calculate these parameters. It is

Manuscript received February 3, 1975.

F. L. Walls is with Time and Frequency Division, National Bureau of Standards, Boulder, Colo. 80302.

A. DeMarchi is with the Time and Frequency Division, National Bureau of Standards, Boulder, Colo. 80302, on leave from the Istituto Elettrotecnico Nazionale, Torino, Italy.

Copyright ©1975 by The Institute of Electrical and Electronics Engineers, Inc.
Printed in U.S.A. Annals No. 509IM003

explicitly assumed that amplitude modulations of the carrier is small compared to phase modulations, which is generally true for precision oscillators.

Specific suggestions for extending the frequency range over which 5-MHz-crystal-controlled oscillators can be used as precision sources are made on the basis of the experimental and theoretical results.

EXPERIMENTAL SYSTEM AND MEASUREMENTS

The experimental system used to study the RF spectrum of precision frequency sources before and after multiplication is schematically shown in Fig. 1. Oscillators 1 and 2 are similar 5-MHz-crystal-controlled oscillators which exhibit excellent short-term stability, $\sim 4 \times 10^{-13}$ at 1 s, and for the purpose of analysis they are assumed to be identical. Spectrum analyzer 1 is used to measure the spectral density of phase fluctuations for the two oscillators at 5 MHz, $S_\phi(5\text{ MHz},f)$ with and without phase modulation added to oscillator 2. Spectrum analyzers 2 and 3 are used to make measurements at 9.2 GHz. The output of mixer 1 is used to make the frequency of oscillator 2 track the frequency of oscillator 1. This loop makes it possible to maintain average phase quadrature at mixers 2 and 3. The unity gain bandwidth of this loop is ~0.1 Hz.

Curve *a* Fig. 2 shows $S_\phi(5\text{ MHz},f)$ for a single oscillator when no extra phase noise is added to oscillator 2. One notes that the dominant contribution to $S_\phi(5\text{ MHz},f)$ for Fourier frequencies between 30 Hz and 30 kHz is white phase modulation, while at the lowest frequencies, flicker of frequency modulation dominates. The decrease of $S_\phi(5\text{ MHz},f)$ for f above 60 kHz is due to filtering in the oscillator and its buffer amplifier. The equations used to calculate $S_\phi(5\text{ MHz},f)$ are

$$S_v(\nu,f) = 2(V_{\text{rms}}(\nu,f)/V_{\text{pp}})^2 \quad (1)$$

and

$S_\phi(\nu,f) = S_v(\nu,f)$ when

$$\Phi_f(\nu) \equiv \int_f^\infty S_\phi(\nu,f)\, df \ll 1 \quad (2)$$

where $S_v(\nu,f)$ is the one sided spectral density of the RF power spectrum center about the carrier frequency ν, as a function of Fourier frequency offset f; $V_{\text{rms}}(\nu,f)$ is the noise voltage at the output of the double balanced mixer 2 (DBM 2) in a 1-Hz bandwidth as a function of Fourier offset f from the carrier at frequency ν; V_{pp} is the sinusoidal peak to peak voltage at DBM 2 when oscillators 1 and 2 differ in frequency [5]. Equations (1) and (2) are valid only when amplitude modulation is insignificant compared to the level of phase modulation and the signals from the two oscillators are approximately in phase quadrature.

The phase noise added to the signal by the multiplier chains can be evaluated by driving both chains by the same source (switch 1 in position *b*) and measuring the resulting $S_\phi^{\text{ch}}(9.2\text{ GHz},f)$ at the output of DBM 3. It is assumed that both multiplier chains contribute equally. In this measurement the phase fluctuations of the source cancel out. It is well known that frequency multiplication by a factor of n increases the magnitude of $S_\phi(\nu,f)$ by a factor on n^2 (i.e., $S_\phi(n\nu,f) = n^2 S_\phi(\nu,f)$) [1], [2]. Therefore, the output phase noise of the chain referred to the input is given by $S_\phi^{\text{ch}}(5\text{ MHz},f) = (1/1836)^2 S_\phi^{\text{ch}}(9.2\text{ GHz},f)$. Curve *b* in Fig. 2 shows the measured phase noise of a single multiplier chain using this technique. The effective input to the multiplier chains is

$$S_\phi^{\text{input}}(5\text{ MHz},f) = S_\phi^{\text{ch}}(5\text{ MHz},f) + S_\phi^{\text{osc}}(5\text{ MHz},f)G^2(f) \quad (3)$$

where $G^2(f)$ describes the frequency dependence of the filtering of input phase noise by the multiplier chain. Curve *c* Fig. 2 shows $S_\phi(9.2\text{ GHz},f)(1/1836)^2$ with switch 1 in position *a*, and no phase noise added to oscillator 2, which is equivalent to measuring $S_\phi^{\text{input}}(5\text{ MHz},f)$ from (3). The good agreement between curves *a* and *c* show that the multiplier chains are broad band compared to the width of the oscillator phase noise spectrum and moreover confirms that the phase noise of the multiplier chains can be neglected. This agreement is crucial to the analysis of the measurements that follow because it verifies that $S_\phi(9.2\text{ GHz},f) = (1836)^2 S_\phi(5\text{ MHz},f)$. Hereafter, the spectral density of phase fluctuations for oscillator 1, and oscillator 2 without added phase noise will be referred to as $S_\phi^0(5\text{ MHz},f)$ and defined by curve *c* Fig. 2.

Fig. 3 shows $S_\phi(5\text{ MHz},f)$ for varying amounts of white phase noise added to oscillator 2. The level of flicker of frequency fluctuation and the 3-dB rolloff frequency of the white phase modulation, 60 kHz, is constant as the level of white phase modulation is increased. This simulates the effect of multiplying the white phase fluctuation portion of $S_\phi^0(5\text{ MHz},f)$ of oscillator 2, which contributes virtually all the phase modulation due to the pedestal, by

$$n_i = \left(\frac{S_\phi^i\ 5\text{ MHz},\ 5\text{ kHz}}{S_\phi^0\ 5\text{ MHz},\ 5\text{ kHz}}\right)^{1/2} \quad (4)$$

where $S_\phi^i(5\text{ MHz},f)$ is the ith level of white phase modulation as noted in Fig. 3. The slope of $S_\phi^i(5\text{ MHz},f)$ is slightly different than the slope of $S_\phi^0(5\text{ MHz},f)$ for f greater than 60 kHz. The importance of this will be discussed later. Fig. 4 shows typical spectrum analyzer traces at 9.2 GHz for varying amounts of white phase noise added to oscillator 2. The resolution is 10 kHz.

The solid dots in Fig. 5 show the measured relative power in the carrier P_c and the pedestal P_p at 9.2 GHz which has been plotted as a function of total simulated multiplication factor $n = 1836\ n_i$ and as a function of the final synthesized frequency $\nu = n_i$ 9.2 GHz (upper scales). The lower scale shows the mean-square phase modulation at 9.2 GHz due to the pedestal $\Phi^p(\nu)$, which is given by

$$\Phi_{(\nu)}{}^p \equiv \int_{\text{pedestal}} S_\phi{}^p(\nu,f)\, df. \quad (5)$$

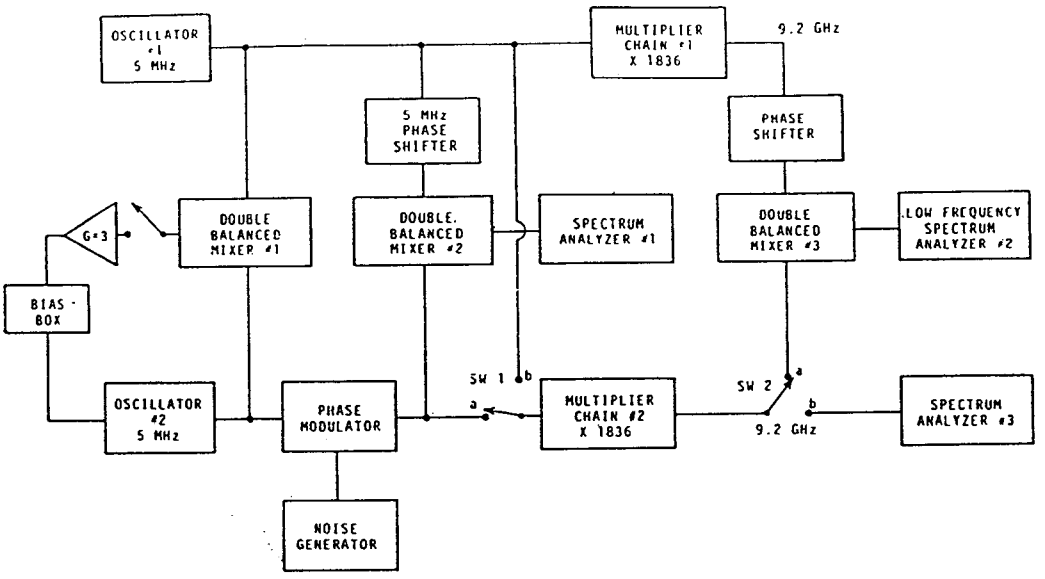

Fig. 1. Block diagram of the experimental system used to study the effect of multiplication on the RF spectrum of an oscillator.

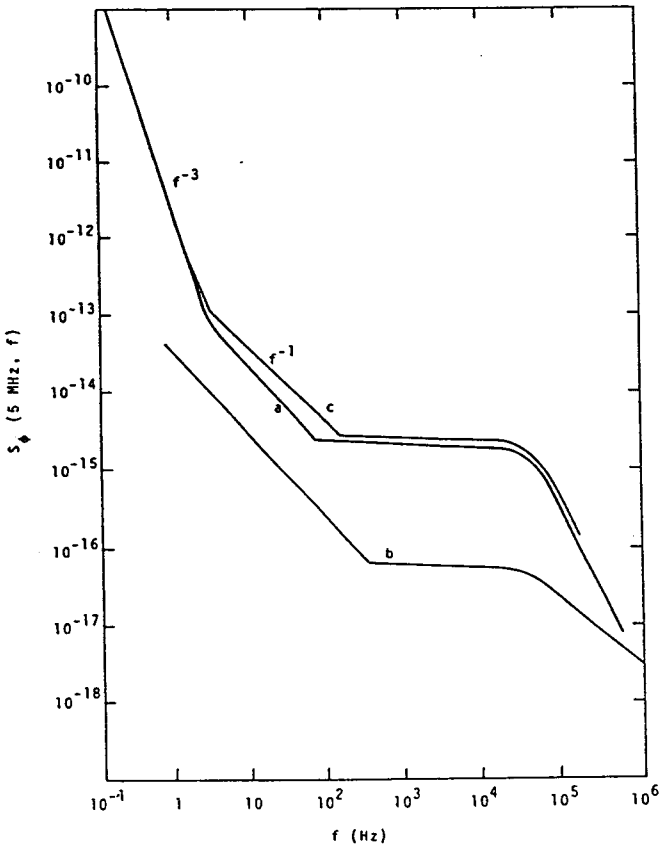

Fig. 2. Spectral density of phase fluctuations. (a) For the 5-MHz crystal controlled oscillators shown in Fig. 1. (b) For the phase noise of the 5-MHz to 9.2-GHz multiplier chains referred to the input. (c) For the output signal at 9.2 GHz divided by the n^2 where n = (9.2 GHz/5 MHz).

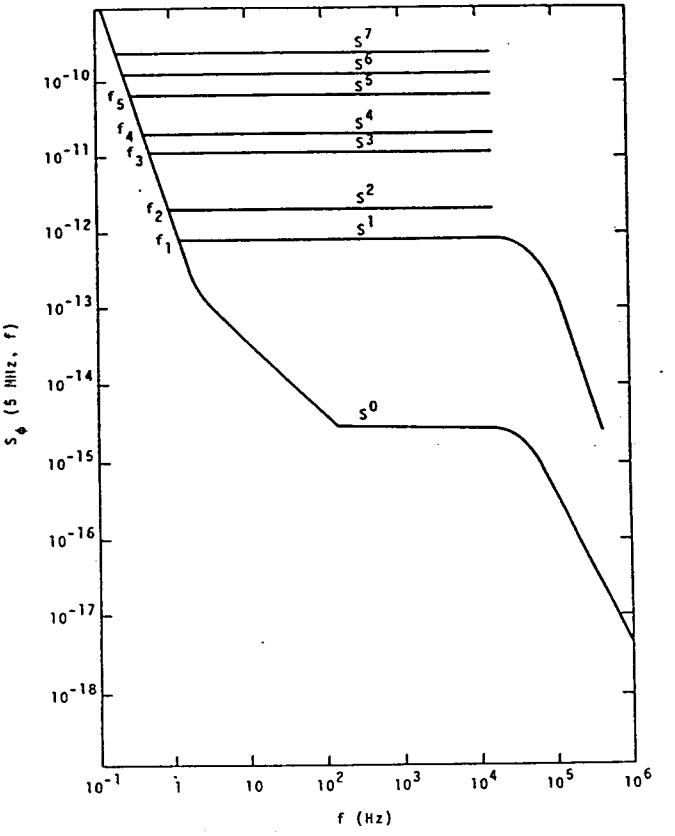

Fig. 3. Spectral density of phase fluctuation for oscillator 2 with various amounts of added phase noise.

For the ith level of white phase fluctuation shown in Fig. 3, $\Phi^p(9.2\text{ GHz})$ is given by

$$\Phi_{i\text{th level}}{}^p(9.2\text{ GHz}) = (1836)^2 \int_{f_i}^{\infty} S_\phi{}^i(5\text{ MHz},f)\, df \quad (6)$$

where the spectrum has been divided between carrier and pedestal as follows.

For carrier

$$S_\phi{}^c(5\text{ MHz},f) = \begin{cases} S_\phi{}^i(5\text{ MHz},f), & 0 < f < f_i \\ 0, & f > f_i \end{cases} \quad (7)$$

For pedestal

$$S_\phi{}^p(5\text{ MHz},f) = \begin{cases} 0, & 0 < f < f_i \\ S_\phi{}^i(5\text{ MHz},f), & f > f_i \end{cases} \quad (8)$$

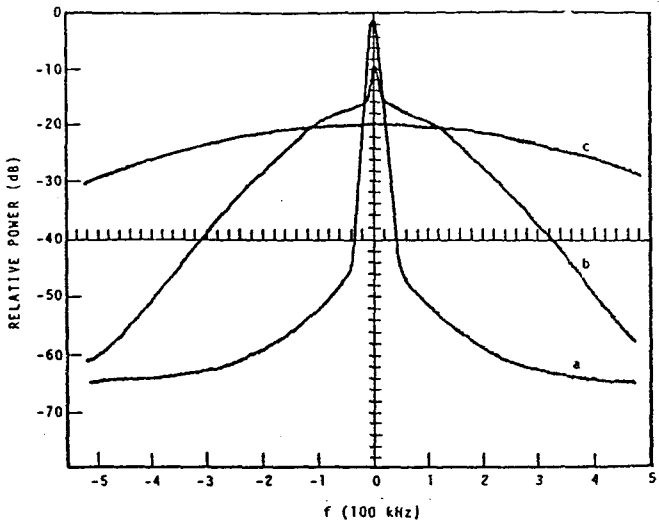

Fig. 4. Typical RF spectrum observed at 9.2 GHz as a function of white noise level. Curve *a* results from the white phase level given by curve s^0 in Fig. 3, curve *b* from the white phase level of curve s^3 in Fig. 3, while curve *c* results from curve s^5 in Fig. 3. Alternately curves *a*, *b*, and *c* can be interpreted as showing the RF spectrum at 9.2 GHz, 500 GHz, and 1.5 THz, due to an input spectrum characterized by curve s^0 in Fig. 3.

and f_i is the frequency at which the ith white phase level intersects the f^{-3} slope of the low-frequency portion of $S_\phi{}^i(5\text{ MHz},f)$.

The open circles in Fig. 5 show the measured height (power) of the noise pedestal in a 1-Hz bandwidth h_p relative to the total power $P_c + P_p = 1$.

The open circles in Fig. 6 show the measured 3-dB linewidth of the noise pedestal as a function of Φ^p and simulated output frequency for the data of Fig. 3. The intercept for $\Phi^p \ll 1$ is just twice the 3-dB linewidth of $S_\phi{}^p(5\text{ MHz},f)$, B_0, shown in Fig. 3. The squares in Fig. 6 show the measured linewidth of the noise pedestal when B_0 is reduced to 6 kHz and $S_\phi{}^p(5\text{ MHz},f)$ rolls off as f^{-2} for $f > 6$ kHz.

SIMPLIFIED CALCULATIONS OF THE RF SPECTRUM

The effect of frequency multiplication on the RF spectrum of a purely phase-modulated signal has been previously treated by Stewart [1], Cutler [2], Middleton [3], and Halford [4]. The distinguishing feature of the work presented here is the emphasis on developing a theory which is 1) expressed in formulas which can be easily evaluated using simple analytical techniques, 2) formulated and easily interpreted in terms of commonly employed experimental measurements, and 3) capable of accurately estimating the relative power in the carrier and the noise pedestal, and the width and shape of the carrier and noise pedestal. In order to achieve this several simplifying approximations are necessary. The range over which the approximations are valid is primarily evaluated from experimental measurements.

The following rigorous expression for the RF spectrum $S_v'(f)$ due to that portion of the phase spectrum lying beyond f_0 is derived in the Appendix

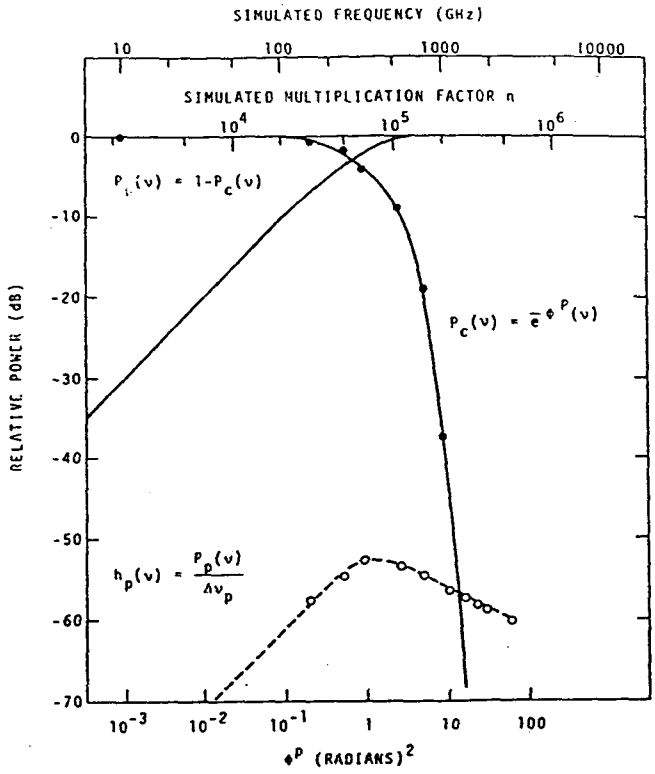

Fig. 5. Measurements of the relative power in the carrier P_c and noise pedestal P_p as a function of total simulated multiplied number referred to 5-MHz input, i.e., $n = 1836\, n_i$, the simulated output frequency ν, and the mean-squared phase modulation at 9.2 GHz due to the noise pedestal Φ^p(9.2 GHz). Also shown is the height h_p or power per hertz in the noise pedestal near the carrier relative to total power $P_c + P_p = 1$. The solid curves are calculated as a function of only the lower scale Φ^p.

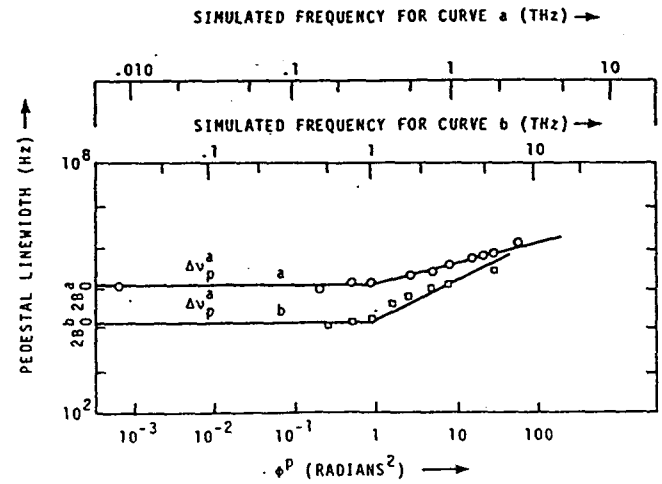

Fig. 6. Dependence of the 3-dB linewidth of the noise pedestal, $\Delta\nu_p$ on $\Phi^p(\nu)$ and the shape of $S_\phi{}^p(\nu,f > B_0)$. Curve *a* and the circles show $\Delta\nu_p(\nu)$ for $S_\phi{}^i(5\text{ MHz},f)$ in Fig. 3 where $S_\phi{}^i(5\text{ MHz},f > B_0) = \alpha K f^{-3}$ and $B_0 = 60$ kHz. Curve *b* and the squares show $\Delta\nu_p$ for $S_\phi{}^i(5\text{ MHz},f > b_0) = K'f^{-2}$ and $B_0 = 6$ kHz.

$$S_v'(\nu,f) = \exp\left[-\Phi_{\phi,f_0}(\nu,0)\right]\left[\delta(f) + S_\phi{}^{f_0}(\nu,f) + \sum_{r=2}^{\infty}\frac{4}{r!}\int_0^\infty \Phi_{\phi,f}{}^r(\nu,\tau)\cos(2\pi f\tau)\,d\tau\right] \quad (9)$$

where

$$\Phi_{\phi,f_0}(\nu,t) = \int_{f_0}^{\infty} S_\phi(\nu,f)\cos(2\pi ft)\,df$$

and

$$S_\phi^{f_0}(\nu,f) = \begin{cases} 0, & f < f_0 \\ S_\phi(\nu,f), & f > f_0. \end{cases}$$

This was derived under the assumption that amplitude modulation is so small as to be unimportant. We expect that $S_v'(\nu,f)$ is a good approximation to the true RF spectral density $S_v(\nu,f)$, for $f > f_0$, i.e., that power at low Fourier frequencies in the spectral density of phase fluctuations do not produce a significant contribution to the voltage spectral density at higher Fourier frequencies. Under this assumption $S_v'(\nu,f) = S_v(\nu,f)$.

When

$$\Phi_{\phi,f_0}(\nu,0) \equiv \Phi_{f_0}(\nu) \ll 1$$

the terms

$$\sum_{r=2}^{\infty} \frac{4}{r!} \int_0^{\infty} \Phi_{f_0}^{\,r}(\nu) \cos 2\pi f\tau \, d\tau$$

can be ignored and one obtains the usual relationship between $S_v(\nu,f)$ and $S_\phi(\nu,f)$, i.e., equation (2). Also the total power in the frequency interval $\nu \pm f_0$ is given by $\exp -\Phi_{f_0}(\nu)$.

When $\Phi_{f_0}(\nu) \geq 1$ the Σ terms contribute some power over the entire spectrum. However, because of the difficulty in evaluating the exact contribution of these terms, which in general requires numerical integration, we will drop them completely and compare only the first two terms of (9),

$$S_c(\nu,f) = \exp\,[-\Phi_{f_0}(\nu)][\delta(f) + S_\phi^{f_0}(\nu,f)] \tag{10}$$

with the experimental data.

Using the first term of (10), the relative power in the carrier P_c and the relative power in the pedestal P_p are given by

$$P_c(\nu) = \exp[-\Phi^p(\nu)] \tag{11}$$

$$P_p(\nu) = 1 - P_c(\nu) \tag{12}$$

where $\Phi^p(\nu)$, the mean-square phase modulation due to the pedestal is given by $\Phi_{f_0}(\nu)$ with f_0 being the dividing line between the carrier and the pedestal as illustrated by the f_i's in Fig. 3. Equations (11) and (12) are plotted in Fig. 5 versus Φ^p(9.2 GHz) in order to compare them with the experimental measurements at 9.2 GHz. The solid curves—as a function of the Φ^p scale—are universal curves in that they can be applied to any RF spectrum where the amplitude modulation is smaller than the phase modulation. The agreement with the experimental points is generally very good until $\Phi^p(\nu)$ becomes so large that the power density in the carrier becomes less than that in the pedestal. For the data of Fig. 4 this occurs at about $\Phi^p = 12$. In the general case it can be shown that the power density in the carrier is equal to that in the pedestal when

$$\Phi^p = \ln \frac{\Delta\nu_p}{\Delta\nu_c} \tag{13}$$

therefore, (11) and (12) are applicable only when

$$\Phi^p(\nu) < \ln \frac{\Delta\nu_p}{\Delta\nu_c} \tag{14}$$

where $\Delta\nu_c$, the linewidth of the carrier, and $\Delta\nu_p$, the linewidth of the pedestal, are calculated below.

The linewidth of the noise pedestal $\Delta\nu_p$ is given by

$$\Delta\nu_p = 2B_0, \quad \text{for } \Phi^p \equiv \int_p S_\phi(\nu,f)\, df < \ln 2 = 0.69 \tag{15}$$

where B_0 is the 3-dB linewidth of the noise pedestal at the input to the multiplier chain.

For $\Phi^p(\nu) > 0.69$ nearly all of the power is in the pedestal whose linewidth can be estimated from the following integral equation

$$\int_{\Delta\nu_p/2}^{\infty} S_\phi^p(\nu,p) = \ln 2 = 0.69, \quad \Phi^p > 0.69. \tag{16}$$

This equation which is derived from the first term of (10) by letting $f_0 = \Delta\nu_p/2$, specifies that one half of the power is contained in the frequency interval $\nu \pm \Delta\nu_p/2$. However, the precise difference between the bandwidth calculated from (16) and the actual 3-dB bandwidth depends on the exact shape of $S_\phi^p(\nu,f)$. When the rolloff of $S_\phi^p(\nu,f)$ for $f > B_0$ varies as $f^{-\alpha}$, then the 3-dB linewidth of $S_v(\nu,f)$ has a particularly simple form which is given in Table I and compared with linewidths from (16) for values of α commonly encountered.

Curve *a* in Fig. 6 shows the linewidth of the pedestal $\Delta\nu_p{}^a$ calculated from (16) and S_ϕ^p(5 MHz,f)—Fig. 3—as a function of Φ^p and ν, which is in good agreement with the measured data points for all values of Φ^p investigated (10^{-10} to 100). The f^{-3} rolloff of S_ϕ^p(5 MHz,f) causes the value of $\Delta\nu_p{}^a$ to vary as $(\Phi^p)^{1/2}$ or ν for $\Phi^p > 1$. When S_ϕ^p(5 MHz,f) was made to rolloff as f^{-2}, then the measured value of pedestal linewidth $\Delta\nu_p{}^b$ varied as Φ^p or ν^2 as indicated by squares in Fig. 6. Curve *b* is the corresponding calculation from (15).

The relative power per hertz in the pedestal is given by

$$S_c(\nu,f) = \begin{cases} 1/(\Delta\nu_p), & f < \Delta\nu_p/2, \quad \Phi^p(\nu) \geq 0.69 \\ S_\phi^p(\nu,f), & f > \Delta\nu_p/2, \\ S_\phi^p(\nu,f), & \Phi^p < 0.69 \end{cases} \tag{17}$$

while the maximum height of the pedestal h_p is approximately given by

$$h_p = \begin{cases} P_p/\Delta\nu_p \\ \Phi^p/2B_0, & \Phi^p \leq 0.69 \\ 1/\Delta\nu_p, & \Phi^p \geq 0.69. \end{cases} \tag{18}$$

The dashed curve Fig. 5 shows the value of h_p calculated from (18) as a function of Φ^p which is in good agreement with the measured data points.

The linewidth of the carrier can be estimated by calculating

$$\Phi_{\Delta\nu/2}{}^c \equiv \int_{\Delta\nu_c/2}^{\infty} S_\phi^c(\nu,f)\, df = 0.69, \quad \Phi^p < \ln \frac{\Delta\nu_p}{\Delta\nu_c} \tag{19}$$

which functionally is identical to (16). The dependence of $\Delta\nu_c$ on commonly encountered forms of $S_\phi^c(\nu,f)$ is therefore given in Table I. Note that $\Delta\nu_c$, at least in the approximation used here, is independent of Φ^p as long as Φ^p is less than ln $(\Delta\nu_p/\Delta\nu_c)$. Curve a in Fig. 7 shows the carrier linewidth $\Delta\nu_c$ corresponding to $S_\phi^c(5\text{ MHz},f)$ in Fig. 3—calculated from (19). In the simulated multiplication process used here only two values of $S_\phi^c(\nu,f)$ are produced namely $S_\phi^c(5\text{ MHz},f)$ and $S_\phi^c(9.2\text{ GHz},f)$ this is because the added noise does not contain significant components at low Fourier frequencies. In both cases the calculated linewidth is infinitesimal compared to the 1-Hz resolution of the spectrum analyzer. This was verified with oscillators 1 and 2 locked and unlocked.

The relative power per hertz in the carrier is given by

$$S_v^c(\nu,f) = \frac{\exp\,[-\Phi^p(\nu)]}{\Delta\nu_c}, \qquad \text{for } f < \Delta\nu_c/2 \quad (20)$$

and

$$S_v^c(\nu,f) = \exp\,[-\Phi^p(\nu)]\,S_\phi^c(\nu,f), \qquad \text{for } f > \Delta\nu_c/2 \quad (21)$$

where $\Delta\nu_c$ is defined by (19). If $\Phi^p > \ln(\Delta\nu_p/\Delta\nu_c)$ then the carrier can no longer be distinguished from the pedestal.

Figs. 4–7 illustrate how the RF spectrum is modified by the multiplication process. The exponential loss of power from the carrier when the mean-square phase fluctuations from the pedestal Φ^p, exceed 1-radian squared is the most serious effect. For the present state-of-the-art commercial 5-MHz-crystal-controlled oscillators, the power is evenly divided between carrier and pedestal at ~300 GHz while at 1 THz the carrier has only −50 dB of the total power.

From the above analysis it is clear that the only way to extend the useful working range of the present 5-MHz oscillator above 1 THz is to reduce the phase modulation due to the pedestal Φ^p. This can be done either by reducing the white phase modulation level of the pedestal or reducing the pedestal bandwidth B_0—either in the oscillator or somewhere along the multiplier chain. Of course changing the pedestal height or width, affect the spectrum in different ways. The importance depends on the bandwidth of the detector compared to the pedestal width. If the detector bandwidth W is larger than B_0, such as commonly used when locking a noisy oscillator to a reference signal, the important parameter is the ratio of power in the pedestal to power in the carrier which for $\Phi^p \ll 1$ is just $P_c/P_p = (1/\Phi^p)$. This is independent of height and width of the pedestal. If W is smaller than B_0 then the carrier to pedestal power ratio is given by $P_c/P_p = (1/\Phi^p)(W/B_0)$ for $\Phi^p \ll 1$. In this case a reduction of Φ^p by decreasing the height of the pedestal is most productive.

Recent measurements and analysis of the inherent short term stability of quartz-crystal resonators [5] indicate that it should be possible to construct 5-MHz-crystal-controlled oscillators with at least 40-dB reduction

TABLE I
Comparison of the linewidth $\Delta\nu$ as a function of the type of noise

$S_\phi(f)$	linewidth $\Delta\nu$ from $\int_{\Delta\nu/2}^{\infty} S_\phi = 0.69$	Actual 3-dB linewidth $\Delta\nu$
$\frac{K_{-2}}{\gamma^2+f^2} \approx \frac{K_{-2}}{f^2}$ White FM	πK_{-2}	πK_{-2}
$\frac{K_{-3}}{\gamma^3+f^3} \approx \frac{K_{-3}}{f^3}$ Flicker FM	$1.70(K_{-3})^{1/2}$	$2.6(K_{-3})^{1/2}$
$\frac{K_{-4}}{\gamma^4+f^4} \approx \frac{K_{-4}}{f^4}$ Random Walk FM	$1.6(K_{-4})^{1/3}$	$\sim 2.8(K_{-4})^{1/3}$

$S_\phi(f)$ is assumed to follow the indicated dependence on f over the entire region of interest. It is necessary to assume that $\gamma > 0$ in order that $\int_0^\infty S_\phi(f)\,df < \infty$.

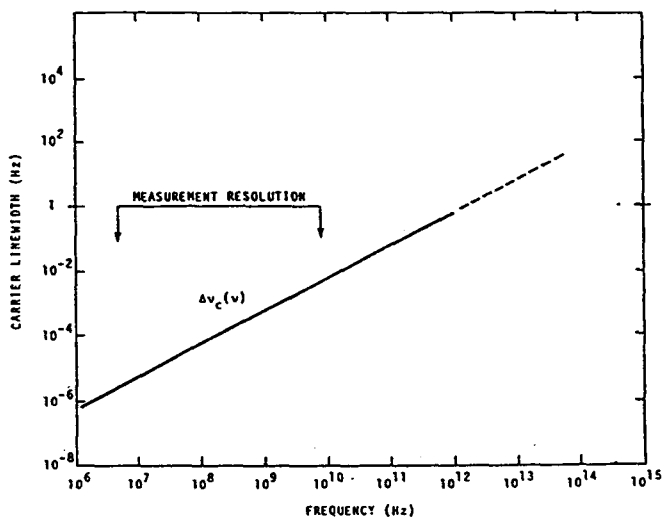

Fig. 7. Calculated linewidth of the carrier $\Delta\nu_c$ for oscillator 1 or 2 as a function of output frequency.

in the white phase level of the pedestal and hence Φ^p. This would provide an oscillator with a possible working range extending to 30 THz without the use of intermediate oscillators or filters. This comfortably overlaps several of the low-frequency lasers commonly used in the far infrared.

The use of high-frequency-crystal-controlled oscillators, e.g., 100 MHz, often provides a signal which has the white phase level 20 dB lower than the present 5-MHz oscillators when compared at the same synthesized frequency. However, the pedestal bandwidth of the high-frequency-crystal-controlled oscillators is much wider so that Φ^p is typically only a factor of 3 to 6 smaller than for the 5-MHz oscillators. Moreover, it has been noted that the flicker of frequency level in quartz crystal resonators and hence crystal-controlled oscillators [5] which determine the carrier line width via (19)

is proportional to the inverse of the crystal Q. Since the product of crystal Q and frequency ν_0 is generally a constant, i.e., $Q\nu_0 \sim 1.2 \times 10^{13}$, a 5-MHz-crystal-controlled oscillator will provide a carrier linewidth approximately 20 times narrower than a 100-MHz-crystal-controlled oscillator. The flicker level of our present oscillators would produce a fast linewidth of ~0.7 Hz at a synthesized frequency of 1 THz. This is over 1000 times narrower than has been achieved to date at 1 THz [6].

The use of a passive filter with a bandwidth of 6 Hz at 9.2 GHz—such as a superconducting cavity filter [7]—would in principle make it possible to multiply the present oscillators to 100 THz without the need for intermediate oscillators. The linewidth would be approximately 70 Hz.

CONCLUSION

A novel experimental technique was described and used to measure the effect of the frequency multiplication process on the RF spectrum of an oscillator. Using this technique it was possible to produce the RF spectrum at 9.2 GHz that would have been produced by frequency multiplying the 5-MHz source to any frequency from 9.2 GHz to 100 THz (10^{14} Hz).

A simplified theory of the multiplication process was developed which allows one to easily calculate the division of power between the carrier and the noise pedestal, the general shape and 3-dB width of the carrier and pedestal for any synthesized frequency. These calculations are made using the measurements of the spectral density of phase fluctuations of the source, the effective input spectral density of phase fluctuations and the bandwidth of the multiplier chain, and the frequency multiplication factor. The calculations agree with the measured results to within the measurement uncertainty of 2 or 3 dB from 5 MHz to 10 THz (10^{13} Hz).

It was shown that the present state-of-the-art commercial 5-MHz-crystal-controlled oscillators are usable as precision oscillators to about 500 GHz without additional filtering whereas with a passive filter 6 Hz wide at 10 GHz they could in principle be used to 100 THz.

The use of 5-MHz-crystal-controlled oscillator with improved short-term stability [5] would, without any additional filtering, have a useful range as a precision source to ~30 THz. The expected linewidth is ~20 Hz. Sources with such spectral purity would make frequency metrology and spectroscopy of unprecedented precision possible throughout much of the far infrared.

APPENDIX

A phase-modulated sinusoidal wave can be described at any instant in the complex form,

$$v(t) = \exp\{j[2\pi\nu t + \phi(t)]\} = \exp j2\pi\nu t\,(z(t)) \quad \text{(A1)}$$

where

$$z(t) = \exp[j\phi(t)]. \quad \text{(A2)}$$

The instantaneous phase $\phi(t)$ is here supposed to be a stationary Gaussian random process with covariance $\Phi_\phi(\tau)$ and power spectra density $P_\phi(f)$

$$P_\phi(f) = \int_{-\infty}^{\infty} \Phi_\phi(\tau) \exp(-j2\pi f\tau)\, d\tau = 2\int_0^{\infty} \Phi_\phi(\tau) \cos(2\pi f\tau)\, d\tau \quad \text{(A3)}$$

$$\Phi_\phi(\tau) = \int_{-\infty}^{\infty} P_\phi(f) \exp(-j2\pi f\tau)\, df = 2\int_0^{\infty} P_\phi(f) \cos(2\pi f\tau)\, df. \quad \text{(A4)}$$

The covariance of $v(t)$ then will be

$$\Phi_v(\tau) = \langle v(t+\tau)v^*(t)\rangle = \exp(j2\pi\nu t)\,\Phi_z(\tau) \quad \text{(A5)}$$

where

$$\Phi_z(\tau) = \exp\{-j[\phi(t) - \phi(t+\tau)]\} = \exp\{-[\Phi_\phi(0) - \Phi_\phi(\tau)]\}. \quad \text{(A6)}$$

The Fourier transform of (A5) gives the RF spectrum of the modulated wave

$$P_v(\nu + f) = P_z(f) = \int_{-\infty}^{\infty} \Phi_z(\tau) \exp(-j2\pi f\tau)\, d\tau. \quad \text{(A7)}$$

Now $\Phi_z(\tau)$ from (A6) can be expanded in powers of $\Phi_\phi(\tau)$ yielding

$$\Phi_z(\tau) = \exp -\Phi_\phi(0) \sum_{r=0}^{\infty} \frac{\Phi_\phi{}^r(\tau)}{r!} \quad \text{(A8)}$$

and so (A2) can be rewritten, also using (A3) and remembering that the covariance is even for τ

$$P_v(\nu + f) = \exp[-\Phi_\phi(0)][\delta(f) + P_\phi(f) + \sum_{r=2}^{\infty} \frac{2}{r!} \int_0^{\infty} \Phi_\phi{}^r(\tau) \cos(2\pi f\tau)\, d\tau]. \quad \text{(A9)}$$

Since in a zero beat measurement one cannot distinguish between the two sides of the spectrum, the single-sided distribution $S_v(\nu,f)$ which contain all the powers included in $P_v(\nu,f)$ is commonly used. $S_v(f)$ is defined as

$$S_v(\nu,f = \begin{cases} 2P_v(\nu + f), & f > 0 \\ 0, & f < 0. \end{cases} \quad \text{(A10)}$$

If we introduce a low-frequency cutoff for $S_\phi(\nu,f)$, so that $S_\phi(\nu,f) = 0$ for $f < f_0$, then the covariance of the phase can be written

$$\Phi_{\phi,f_0}(\tau) = 2\int_{f_0}^{\infty} P_\phi(f) \cos(2\pi f\tau)\, df = \int_{f_0}^{\infty} S_\phi(\nu,f) \cos(2\pi f\tau)\, df \quad \text{(A11)}$$

and (A9) becomes

$$S_v'(\nu,f) = \exp[-\Phi_{\phi,f_0}(0)][\delta(f) + S_\phi(\nu,f) + \sum_{r=2}^{\infty} \frac{4}{r!} \int_0^{\infty} \Phi_{\phi,f_0}{}^r(\nu,\tau) \cos(2\pi f\tau)\, d\tau. \quad \text{(A12)}$$

ACKNOWLEDGMENT

The authors wish to acknowledge the many helpful suggestions of S. Jarvis, Jr., H. Hellwig, D. W. Allan, A.

E. Wainwright, and D. J. Glaze. One of us (A. DeMarchi) wishes to express his appreciation to the National Bureau of Standards for the opportunity to participate in this Research as a Guest worker and to his home institution—The Istituto Elettrotecnico Nazionale—for its continued support.

REFERENCES

[1] J. L. Stewart, "The power spectrum of a carrier frequency modulated by Gaussian noise," *Proc. IRE*, vol. 42, pp. 1539–1543, 1954.
[2] L. S. Cutler, "A frequency standard of exceptional spectral purity and long term stability frequency," vol. 1, pp. 20–27, 1962.
[3] D. Middleton, *Introduction to Statistical Communication*. New York: McGraw-Hill, 1960.
[4] D. Halford, "Infrared–microwave frequency synthesis design: Some relevant conceptual noise aspects," *Proc. Frequency Standards and Metrology Seminar*, pp. 431–466, 1971 (available from Department of Electrical Engineering, Laval University, Quebec, Canada).
[5] F. L. Walls and A. E. Wainwright, "Measurement of the short term stability of quartz crystal resonators and the implications for crystal oscillator design and applications," *IEEE Trans. Instrum. Meas.*, vol. IM-24, pp. 15–20, Mar. 1975.
[6] J. S. Wells, D. G. McDonald, A. S. Risley, S. Jarvis, Jr., and J. D. Cupp, "Spectral analysis of a phase locked laser at 891 GHz, an application of Josephson junctions in the far infrared," *Rev. Phys. Appl.*, vol. 9, pp. 285–292, Jan. 1974.
[7] J. P. Turneaure, "The status of superconductivity for RF applications," presented at 1972 Applied Superconductivity Conf., Anapolis, Md. See also J. L. Stone and H. W. Hartwig, "Performance of superconducting oscillators and filters," *J. Appl. Phys.* vol. 39, pp. 2665–2671, 1968.